The absorbing boundary method. III. Tunneling decay and scattering resonances

George Bacskay and Sture Nordholm

Citation: The Journal of Chemical Physics **72**, 2120 (1980); doi: 10.1063/1.439307
View online: http://dx.doi.org/10.1063/1.439307
View Table of Contents: http://scitation.aip.org/content/aip/journal/jcp/72/3?ver=pdfcov
Published by the AIP Publishing

The absorbing boundary method. III. Tunneling decay and scattering resonances

George Bacskay and Sture Nordholm

Department of Theoretical Chemistry, University of Sydney, Sydney, N. S. W. 2006, Australia
(Received 17 April 1979; accepted 30 April 1979)

The recently developed absorbing boundary method (ABM) is applied to the calculation of tunneling decay rates and corresponding shape resonances in the scattering cross section. The analysis is carried out in terms of the contribution to the density of states from the resonant region of the spatial domain. One-dimensional test calculations have been carried out using the ABM and several related continuum state methods. While the ABM produces practically useful predictions for the location and shape of the resonance lines, it cannot in its present forms match the accuracy of the best continuum state methods. We have compared results obtained by the ABM (SMA and ISMA), the R-matrix method, the recently developed CGFEM and Bloch corrected R-matrix method, the stabilization method of Hazi and Taylor, and a simple pseudo bound state method.

I. INTRODUCTION

It is well known that the quantum theory of dissociation/ionization or scattering phenomena is made more difficult by the fact that the relevant region of energy falls into the continuous part of the spectrum of the Hamiltonian of the system. The difficulty is particularly acute from a computational point of view. As a consequence many attempts have been made to develop theories of continuum processes in such a way that no explicit reference to the continuum of energy eigenfunctions is made. The aim, of course, is to allow all necessary calculations to be carried out within a space spanned by a discrete set of basis functions. There are a large number of such theories some of which are in widespread use.[1-4]

The present work is concerned with a class of continuum processes distinguished by the fact that they proceed at least partially by a nonclassical tunneling mechanism. This class can again be subdivided into two subclasses the former containing tunneling decay or transfer processes as are well known in the theory of unimolecular reactions[5-7] and the latter containing resonant scattering processes.[8-10] There is, as will be clearly illustrated below, a very close connection between these two subclasses of continuum phenomena. The resonant part of the scattering process is essentially a continuous sequence of association–dissociation events. Upon time-reversal association becomes dissociation and vice versa. The experimental manifestation of such resonant potential barrier penetration takes the form of so-called shape resonances in the scattering cross sections.

The main aim of the present work is to illustrate how our recently developed absorbing boundary method (ABM)[11-13] can be applied to the prediction of tunneling decay rates and scattering resonances and to obtain an understanding of its accuracy when applied to such processes. The ABM allows quantum dynamics on open domains to be resolved by finite basis set methods. The method has been shown capable of high numerical accuracy in test calculations involving mainly classically allowed decay mechanisms.[12] Although an examination of the derivation of the ABM indicates it is conceptually sound for tunneling processes as well, it is more difficult to predict its quantitative accuracy, particularly in view of the great sensitivity of these processes to the shape of the potential. Another factor motivating our independent examination of tunneling processes is the breakdown of the global method used in earlier work[12] on the basis that it provides a nearly exact description of the bulk of the classically allowed decay. This method becomes inaccurate for long times and therefore cannot resolve the slow tunneling processes.

It is generally the case that information concerning very slow processes is more readily available in the energy dependence rather than in the time dependence. Thus we shall approach tunneling processes from the point of view of scattering theory rather than decay rate theory. This will also allow us to establish a connection between these two theoretical approaches. The time-dependent reactant probabilities examined in our previous work[12] will be replaced below by the line shapes of the corresponding reactant states. It is well known that narrow shape resonances give rise to Lorentzian line shapes which can be conveniently determined by the corresponding Breit–Wigner[14] resonance in the energy dependence of the scattering phase shift. We will, however, find it convenient to develop an alternative analysis based on the energy dependence of the density of states which appears to offer significant advantages.

In order to evaluate the accuracy of the ABM we need, of course, to have available more accurate predictions for the purpose of comparison. We have chosen to relate our test calculations to those performed earlier by Hazi and Taylor[15] while investigating the accuracy of the stabilization method[16,17] which has since become a standard means for predicting locations and widths of scattering resonances. The stabilization method is of particular interest because it is a finite basis set method and, as we shall see below, it is based on distinctive features of quantum dynamics which may not yet be fully appreciated. We shall offer a brief analysis of this method and examine a number of alternative methods including the R-matrix method,[2] several recent improvements on the R-matrix method[18,19] closely connected with the ABM, and a very simple global resonance method[20] comparable to the global method used in our earlier investigation of time dependence.[12]

 0021-9606/80/032120-11$01.00

II. THEORETICAL APPROACH TO TUNNELING DECAY AND SCATTERING RESONANCES

A. Tunneling decay

Let us first recall the basic features of the ABM as described in detail in preceding articles.[11,12] The configuration space of the system whose decay we shall study is divided into an interior and an exterior part, the latter being of infinite extent. On the assumption that the decay from the interior region is irreversible an approximate effective Hamiltonian,

$$H_{eff} = H_B - iH_D \ , \tag{1}$$

which includes a dissipative term accounting for the decay, $-iH_D$, is obtained. The effective Hamiltonian operates only on functions on the interior domain and can be used to obtain the time dependence of wave functions on the interior by the usual bound state methods. That is, if the projection operator P projects out the subspace of functions on the interior domain and the wave function ψ is initially on the interior domain,

$$P\psi(0) = \psi(0) \ , \tag{2}$$

then the time dependence of the projected part can be estimated as

$$P\psi(t) = \exp(-itH_{eff}/\hbar)\psi(0) \ . \tag{3}$$

In other words we have

$$P\exp(-itH/\hbar)P \simeq \exp(-itH_{eff}/\hbar) \ . \tag{4}$$

It should be clear that (3) and (4) allow determination of the rate of decay from the interior domain. This would be particularly easy if H_{eff} were in diagonal form in which case one finds

$$P\psi(t) = \sum_{l=1}^{\infty} c_l \exp[-it(E_l - i\lambda_l)/\hbar]\psi_l \ , \tag{5}$$

where $\{\psi_l\}_1^\infty$ is the set of eigenfunctions of H_{eff},

$$H_{eff}\psi_l = (E_l - i\lambda_l)\psi_l \ . \tag{6}$$

This set is discrete because the interior region is of finite extent. Thus it is possible to work with a finite basis set as long as the relevant range of eigenfunctions of H_{eff} can be accurately reproduced in this basis set. It must be noted that H_{eff} is generally a nonnormal operator. It follows that the eigenfunctions are linearly independent but not orthogonal, in general. Note also that an eigenfunction of H_{eff} decays according to

$$\langle P\psi(t) | P\psi(t)\rangle = \langle P\psi(0) | P\psi(0)\rangle \exp(-2\lambda_l t/\hbar) \ , \tag{7}$$

i.e., exponentially with the rate coefficient given by

$$k_l = 2\lambda_l/\hbar \ . \tag{8}$$

Specializing now to the case of decay by a tunneling mechanism we first note that it is necessary to extend the interior region far enough so that all potential barriers which can give rise to reflection are contained in the region. Naturally enough reflection off barriers in the exterior region may lead to backflow, seriously violating the assumption of irreversible decay. Secondly, we note that tunneling decay is generally very slow. As will be shown below this means that there is, to a good approximation, a single well defined eigenstate of H_{eff} corresponding to each resonance in either the tunneling decay as a function of energy or the scattering cross section as a function of energy. This state is very nearly orthogonal to all other eigenstates of H_{eff} and decays exponentially with a rate coefficient related to the imaginary part of the eigenvalue as shown in (6)–(8). Thus, sufficiently slow tunneling gives rise to isolated resonances which are particularly simple to identify. More generally one must allow for the possibility of overlapping resonances[21–23] which are more likely to occur the more rapid the decay is, or the more dense the spectrum of eigenvalues of H_{eff} is. It is then necessary to work with the full propagator as in (4) rather than with isolated eigenstates and the nonorthogonality of the eigenstates cannot be neglected. The decay of any pure state can, of course, be obtained from (5) and in the case of a mixed state described by the density matrix $\rho_p(t)$ the time dependence can be obtained from

$$\rho_p(t) = \exp(-itH_{eff}/\hbar)\,\rho_p(0)\exp(itH_{eff}^\dagger/\hbar) \ , \tag{9}$$

where

$$H_{eff}^\dagger = H_B + iH_D^\dagger \ . \tag{10}$$

B. Scattering resonances

As noted in the introduction there are significant advantages in studying very slow decay processes such as tunneling decay in the energy domain rather than directly in the time domain as we have done before. It is only natural that by approximate methods one would find it easier to examine energy dependence over a very narrow interval rather than time dependence over very long periods of time. Moreover, a change from the time to the energy domain will bring us closer to traditional methods of scattering theory with which we wish to compare. Our aim is not only to examine the accuracy of the ABM as applied to tunneling decay but also to show how this method derived in the time domain readily produces results in the energy domain normally obtained by some form of energy dependent scattering theory.

In this work we are concerned in particular with the so-called shape resonances in the scattering cross section. As already noted these resonances are directly related to tunneling decay through a potential barrier. Traditionally shape resonances in the scattering cross section are predicted on the basis of an analysis of the phase shift as a function of energy.[14] The cross section can be expressed in terms of the phase shifts and in the case of an isolated resonance the Breit–Wigner one-level approximation yields the following expression for the phase shift as a function of energy,[15]

$$\eta(E) = \eta_{pot}(E) + \tan^{-1}\left(\frac{\Gamma/2}{E_r - E}\right) \ . \tag{11}$$

Here $\eta_{pot}(E)$ is a background phase shift, expected to vary smoothly with E, and the second term on the right is the resonant part of the phase shift. E_r is the location of the resonant state in the energy spectrum and Γ is a width parameter. The resonant contribution to the cross section behaves like

$$\Delta\sigma_r(E) = \frac{4\pi(2l+1)}{k^2}\,\frac{\Gamma^2}{4(E-E_r)^2 + \Gamma^2} \tag{12}$$

in the case of potential scattering[14] where l is the angular momentum and k the magnitude of the wave vector. For a spherically symmetric potential the problem is effectively one-dimensional and following Hazi and Taylor[15] we shall limit our present test calculations to one dimension. As we shall see below the Breit–Wigner approximation implies exponential decay of the resonance state with a rate coefficient equal to $\Gamma/\hbar$. Thus tunneling decay rates and isolated shape resonances have, in the past, been determined by fitting the calculated phase shifts at energies close to the resonance to a parametrized Breit–Wigner functional form.[8,24,25]

In the present work we shall deviate from the usual phase shift analysis and develop instead an alternative analysis based on the density of states. As is well known from the work on quantized second virial coefficients in statistical mechanics[26] there is a close connection between the phase shifts and the density of states. We have

$$\rho(E) = \rho^{(0)}(E) + \frac{1}{\pi}\frac{d\eta(E)}{dE} , \tag{13}$$

where $\rho^{(0)}(E)$ is the density of states in the absence of the potential and the second term is the change due to the presence of the potential. It is assumed here that the potential is of finite range and we note that $\rho^{(0)}(E)$, $E > 0$, is infinite if no cutoff is imposed on the domain. From the Breit–Wigner formula (11) one then finds the following expression for the density of states in the presence of an isolated resonance,

$$\rho(E) = \rho^{(0)}(E) + \Delta\rho_{\text{pot}}(E) + \Delta\rho_r(E) , \tag{14}$$

where the change due to the potential has been split into a smooth background part, $\Delta\rho_{\text{pot}}(E)$, and a resonant part, $\Delta\rho_r(E)$. The latter term can be given explicitly as

$$\Delta\rho_r(E) = \frac{1}{\pi}\frac{\Gamma/2}{(E-E_r)^2 + (\Gamma/2)^2} , \tag{15}$$

where E_r and Γ are the location and width parameters of the Breit–Wigner formula. Identifying $\Delta\rho_r(E)$ with the contribution to the total density of states due to the isolated resonance state we note that the line shape is Lorentzian. The same line shape occurs in the expression (12) for the contribution of the resonance to the cross section. Thus it is clear that the resonance in the cross section can be interpreted as being due entirely to a similar resonance in the density of states.

We have now established a basis for the analysis of scattering resonances in terms of contributions to the density of states. While the density of states analysis appears to be as sound as the traditional phase shift analysis there are still problems with both approaches. One problem shared by both approaches concerns the need to unambiguously separate the resonant from the nonresonant contribution to the cross section. This problem, as well as the validity of the entire one-level analysis discussed above, becomes more difficult as the width of the resonance increases. However, in the case of the density of states analysis there is a natural solution to this problem. The basic idea is that the resonance effects can be associated with finite subdomains which are generally easily identified. Consider the simple one-dimensional potential with a barrier shown in Fig. 1. In this case it is clear that the scattering resonances are due to states trapped behind the top of the potential barrier. Thus we split the total density of states into two parts,

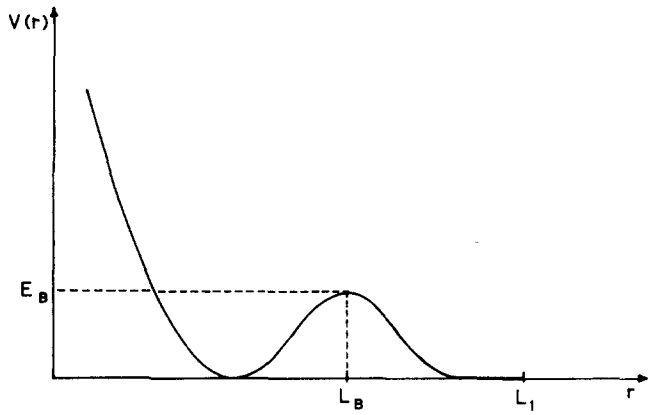

FIG. 1. Typical one-dimensional potential giving rise to tunneling decay scattering resonances.

$$\rho(E) = \rho_{[-\infty, L_B]}(E) + \rho_{[L_B, \infty]}(E) \tag{16}$$

and identify the contribution from the region $[-\infty, L_B]$ behind the barrier as the resonant part,

$$\Delta\rho_r(E) = \rho_{[-\infty, L_B]}(E) \tag{17}$$

and that from the region outside the top of the barrier as the background part. We can now look for Lorentzian resonances in $\rho_{[-\infty, L_B]}(E)$ for $E < E_B$, having eliminated essentially all of the nonresonant part of the problem not involving tunneling in a fundamentally correct manner.

We shall now show how one can use the ABM to obtain the contribution to the density of states from a subspace corresponding to the projection operator B. It will be assumed that this subspace is contained within the subspace corresponding to the projection operator P used in the derivation of the ABM. The contribution of B space to the total density of states $\rho(E)$ can then be obtained from the relation

$$\rho_B(E) = \mathrm{Tr}[B\delta(H-E)] . \tag{18}$$

Rewriting the δ function as a Fourier transform we get

$$\rho_B(E) = (2\pi\hbar)^{-1}\int_{-\infty}^{\infty} dt\, \mathrm{Tr}[B\exp(-it(H-E)/\hbar)]$$

$$= (\pi\hbar)^{-1}\,\mathrm{Re}\int_0^{\infty} dt\, \mathrm{Tr}[B\exp(-it(H-E)/\hbar)B] . \tag{19}$$

Noting that B space is contained in P space we can use the projected propagator in the ABM approximation [see (4)] to get

$$\rho_B(E) = (\pi\hbar)^{-1}\,\mathrm{Re}\int_0^{\infty} dt\, \mathrm{Tr}[B\exp(-it(H_{\text{eff}}-E)/\hbar)B] . \tag{20}$$

The actual calculation of $\rho_B(E)$ is readily carried out by use of an orthonormal basis $\{\phi_l\}_1^M$ spanning a subspace containing B space. Recalling (6) and using the notation

$$\langle\phi_l|\psi_n\rangle = Q_{ln} , \quad \langle\phi_l|B|\phi_n\rangle = B_{ln} , \tag{21}$$

$$|\phi_l\rangle = \sum_{n=1}^{N} R_{nl} |\psi_n\rangle \ , \tag{22}$$

where we have assumed that the orthonormal basis is contained in P space we get

$$\rho_B(E) \simeq \mathrm{Re} \sum_{l=1}^{M} \sum_{n=1}^{M} \sum_{m=1}^{M} \sum_{j=1}^{N} B_{ln} Q_{nj} \frac{1}{\pi} \frac{1}{\lambda_j + i(E_j - E)} R_{jm} B_{ml} \ . \tag{23}$$

This result can be simplified to

$$\rho_B(E) \simeq \mathrm{Re} \sum_{j=1}^{N} F_j \frac{1}{\pi} \frac{1}{\lambda_j + i(E_j - E)} \ , \tag{24}$$

where

$$F_j = \sum_{l=1}^{M} D_{jl} A_{lj} \ , \tag{25}$$

$$A_{lj} = \sum_{n=1}^{M} B_{ln} Q_{nj} \ , \tag{26}$$

$$D_{jl} = \sum_{m=1}^{M} R_{jm} B_{ml} \ . \tag{27}$$

It can be seen from the results above that after diagonalization of H_{eff} the contribution to the density of states from any subspace of P space can be obtained as a function of energy at little extra effort. Below we shall be concerned with potentials of the kind shown in Fig. 1 and B space will be taken as all functions on the interval $[-\infty, L_B]$, i.e., to the left of the potential barrier. In order to make the problem numerically tractable we must also truncate the basis set to a finite and manageable number of states. This corresponds to a truncation of the range of energy over which we can accurately calculate $\rho_B(E)$.

C. The global resonance method

The main purpose of this work is to examine the accuracy of the ABM as applied to very slow decay proceeding by tunneling through a potential barrier. To this end we shall use the ABM to calculate $\rho_B(E)$ as discussed above. In order to establish the accuracy of the ABM we shall compare its results for the location and width of the shape resonance to corresponding predictions obtained from other more specialized and presumably more accurate methods. Noting the utility of our simple global method in the preceding time-dependent calculations[12] we now develop a similar method for our present calculation of $\rho_B(E)$.

We start from (18) and specialize to one-dimensional systems. A projection operator B is defined by

$$\begin{aligned} B\phi(r) &= \phi(r) \ , \quad L_0 \le r \le L_B \ , \\ &= 0 \ , \qquad r > L_B \ . \end{aligned} \tag{28}$$

If we use the energy eigenfunction basis (18) can be rewritten as (see the Appendix)

$$\rho_B(E) = \int_{L_0}^{L_B} dr\, \rho(E) \, |S(E,r)|^2 \ . \tag{29}$$

Here $\rho(E)$ is the total density of states. Strictly speaking $\rho(E)$ is infinite and $S(E,r)$ vanishes but if we relax the normalization constraint and choose $S(E,r)$ such that

$$S(E,r) = \sin[(2mE)^{1/2}/\hbar + \theta(E)] \ , \quad r \to \infty \ , \tag{30}$$

then $\rho(E)$ is given by

$$\rho(E) = (2m/E)^{1/2}/\hbar\pi \ . \tag{31}$$

We have assumed here that we are in the continuous part of the spectrum and the range of the potential is finite. In that case $\rho(E)$ is independent of the potential and all of the nontrivial structure of $\rho_B(E)$ is contained in the form of the eigenfunction $S(E,r)$ for small r where the potential is nonvanishing.

Suppose now that we choose L_1 such that the potential to a good approximation can be taken to vanish for $r \ge L_1$. If we then introduce a finite basis set on the interval $[L_0, L_1]$, where each basis function vanishes at L_0 and L_1, and diagonalize the Hamiltonian in this basis we will get a sequence of bound states. As long as L_0 is properly located in the classically forbidden part of the potential barrier on the extreme left in Fig. 1 each such bound state at energy $\hat{E}_l$ will, in fact, be a good approximation to the continuum eigenfunction at the same energy for $L_0 < r < L_1$. Close to L_1 the pseudobound state will behave like a sine function,

$$\hat{S}_l = A_l \sin\{[(2m\hat{E}_l)^{1/2} r/\hbar] + \theta_l\} \ , \quad r \lesssim L_1 \ . \tag{32}$$

Here $|A_l|$ can be obtained from

$$\frac{d}{dr} \hat{S}_l(r) = A_l[(2m\hat{E}_l)^{1/2}/\hbar] \cos\{[(2m\hat{E}_l)^{1/2} r/\hbar] + \theta_l\}, \quad r \lesssim L_1 \tag{33}$$

with a particularly simple result when $r = L_1$. Thus we can obtain the value of $\rho_B(E)$ at the energies $\{\hat{E}_l\}$ from the relation

$$\rho_B(E) = |A_l|^{-2} [(2m/\hat{E}_l)^{1/2}/\hbar\pi] \int_{L_0}^{L_B} dr \, |\hat{S}_l(r)|^2 \ . \tag{34}$$

By changing the location of L_1 we can increase the number of points at which $\rho_B(E)$ is known. Thus it is generally possible to map out $\rho_B(E)$ by some convenient interpolation method after a few bound state diagonalizations with a varying L_1. One may also keep L_1 fixed but vary the boundary condition at L_1 or use some combination of these two procedures. It is, of course, true that this method of obtaining $\rho_B(E)$ which we shall call the global method does not readily allow us to predetermine the energies at which we will obtain $\rho_B(E)$. In the case of resonances this is, however, an advantage since each calculation will tend to produce one eigenvalue close to the peak of any given resonance line. Thus the likelihood that a resonance will be overlooked is practically zero. This advantage is also present in the case of the ABM procedure discussed above and it eliminates a problem which can be quite serious using other methods in cases when the resonances are very narrow. Since the line shape is then Lorentzian to a very good approximation, one can readily obtain E_r and Γ in (15) from a few values of $\rho_B(E)$ for energies close to E_r.

D. The stabilization method

A frequently used method bearing some resemblance to the global resonance method described above is the stabilization method developed by Taylor and co-

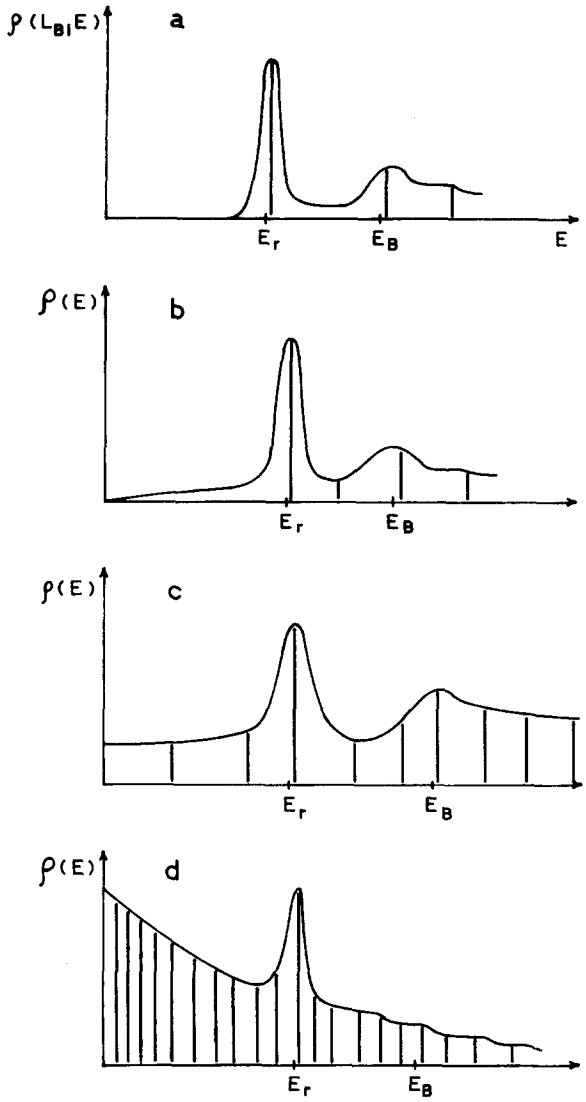

FIG. 2. Contribution to the total density of states from the region $(-\infty, L)$ for increasing L. Estimated locations of eigenvalues from a finite basis set diagonalization scheme are also shown.

workers[16,17] and investigated in detail by Hazi and Taylor.[15] We have found the latter work relevant not only because it has provided a convenient reference frame for our own test calculations but also because the stabilization method relies upon a peculiarly quantum mechanical phenomenon which may play a role in many types of rate processes. Still, it appears that this phenomenon is as yet not well known. A simple analysis will be given below.

Referring the reader to the literature for a detailed description of the stabilization method[15,16] we restrict ourselves here to an abbreviated analysis of several aspects of particular relevance to our own work. We note first that there is a significant difference in the choice of basis functions in the work of Hazi and Taylor and our own work. We have consistently used a sine function basis. The advantage of such a choice apart from numerical tractability is that the spatial domain of resolution is well defined and the energy range resolved is also readily assessed. The importance of these features of the sine function basis set can be understood from the following physical explanation of the stabilization method. Let us consider the contribution to the total density of states from the region $[-\infty, L]$, $\rho(L; E)$. For $L = L_B$ and $E < E_B$ (Fig. 1) we expect $\rho(L; E)$ to consist of one or more Lorentzian lines with no smooth background. As we increase L beyond L_B we expect a smooth background to appear as indicated in Fig. 2. The diagonalization of the Hamiltonian in a sine function basis set on $[L_0, L]$ (where L_0 is properly located in the classically forbidden region on the left) will produce an approximate discretization of $\rho(L; E)$,

$$\rho(L; E) \simeq \tilde{\rho}(L; E) = \sum_{l=1}^{N(L)} \delta(E - E_l(L)) \ . \tag{35}$$

The location of the pseudobound state energy eigenvalues $\{E_l(L)\}_1^{N(L)}$ will reflect the underlying probability density $\rho(L; E)$. Thus it would be possible to recover $\rho(L; E)$ from $\tilde{\rho}(L; E)$ to some accuracy depending on the amount of structure in $\rho(L; E)$ by applying a smoothening procedure to $\tilde{\rho}(L; E)$. In fact, the Stieltjes imaging method developed by Langhoff and co-workers[27] can be understood in these terms.[28] In this case one starts from a discretized photoionization cross section and produces a smooth cross section but the basic principles are the same as above. The imposition of a particular type of boundary condition at $r = L$ does affect the location of the eigenvalues to some extent but this problem rapidly diminishes as L grows. The interpretation of $\rho(L; E)$ as a probability density for the location of eigenvalues $E_l(L)$ implies that any interval $[E_1, E_2]$ such that

$$\int_{E_1}^{E_2} dE\, \rho(L; E) \simeq 1 \tag{36}$$

is nearly certain to contain a single level. As a consequence, for $L \geq L_B$ there will be at least one level within $\sim \gamma$ of E_r. The occurrence of two or more levels within Γ of E_r can arise due to two fundamentally different causes:

(1) Accidental near degeneracy: In this case diagonalization of the Hamiltonian on the interval $[L_B, L]$ produces an eigenvalue within Γ of E_r as does the diagonalization of H on $[L_0, L_B]$. Once the boundary condition at $r = L_B$ is removed these two states will, of course, couple and the energy gap widen somewhat, but if the coupling is weak the two global eigenvalues may still both remain within Γ of E_r. The term accidental near degeneracy applies because the energy gap between the levels on $[L_B, L]$ is much larger than Γ at energies around E_r. Thus a further increase in L will break the near degeneracy leaving only a single "stable" state within Γ of E_r. The ultimate near degeneracy occurs when the potential on the interval $[L_0, L]$ forms a symmetric double well potential in which case the left and right local energy eigenvalues are perfectly matched.[29,7] In general, however, the double well potential is asymmetric and the mismatch in left and right local energies is sufficient to prevent any significant coupling. Thus the global levels below the barrier height E_B remain left or right localized. Since the increase in L only changes the right well the left localized eigenstates will appear to be "stable."

TABLE I. Results of stabilization calculation for the HT potential ($\lambda = 0.260$) using a sine function basis (N = number of functions) on the interval $[-5.0, L]$. The four eigenvalues from the set $\{E_l\}$ that are closest to the resonance energy of 0.4290 are listed with the corresponding interior norms I_l.

N	L	l	E_l	I_l
20	8.0	1	0.1853	0.1282
		2	0.4266	0.9628
		3	0.6352	0.4922
		4	1.0731	0.6500
40	21.0	4	0.2377	0.0561
		5	0.3620	0.1673
		6	0.4313	0.8443
		7	0.5259	0.1742
60	34.0	8	0.3212	0.0625
		9	0.3983	0.2597
		10	0.4354	0.6943
		11	0.5031	0.1202
80	47.0	12	0.3596	0.0713
		13	0.4128	0.3895
		14	0.4394	0.5189
		15	0.4932	0.0961
100	60.0	16	0.3815	0.0894
		17	0.4201	0.4917
		18	0.4431	0.3700
		19	0.4876	0.0813

(2) Destabilization: As L increases the density of states on the interval $[L_B, L]$ increases roughly linearly with L until the energy gap at energies around E_r becomes comparable to Γ. Then there will always be at least two local levels within Γ of E_r and we may say that the resonance line has been resolved when

$$\rho_{[L_B, L]}(E_r)\,\Gamma > 1 \ . \tag{37}$$

If the resonance is very narrow L would have to be very large for destabilization to occur and it may be practically impossible to resolve the corresponding line in a finite basis set calculation. This is the situation to which the stabilization method applies.

In order to illustrate the arguments above we show in Table I selected results from a stabilization calculation using a sine function basis set for the Hazi and Taylor potential with the most narrow barrier ($\lambda = 0.260$). It can be seen that for L not much larger than L_B there is a single stable state within Γ of E_r and localized on the interior. When L is increased to about 50 the exterior density of states has become large enough that the resonance has become split between two states and for $L \simeq 100$ we would expect it to be spread over four states and so on.

While it would appear that the destabilization illustrated in Table I would be a serious problem encountered when using the stabilization method one must recognize that this problem is likely to affect only broad resonances. Moreover, the ability to resolve a resonance line and thus destabilize the corresponding stable state depends strongly on the basis set used. The sine function basis we have used is nearly optimal in this regard. If N, the number of basis functions, is kept proportional to the length of the interval as L grows then the energy range remains roughly constant and all of the extra basis functions are used to increase the total density of states in the relevant low energy range. The harmonic oscillator basis functions used by Hazi and Taylor are far less likely to produce destabilization. This is because as N increases both the energy and the spatial ranges increase, the latter only slowly with N. One would need roughly 1000 such basis functions to resolve the resonance studied in Table I to the extent that we have resolved it using 100 sine basis functions. From the point of view of the stabilization method where one does not want to resolve the stable state it may then seem as if the harmonic oscillator basis set is to be preferred due to its natural tendency to produce stability. However, it must be noted that it is the contrast between stable and unstable states which allows the resonance to be determined. Thus a basis set which merely increased the energy range as N increased would, in fact, not be able to distinguish between stable and unstable states. All states not at the top of the energy range would be stable. Thus the lack of contrast between stable and unstable states may be a problem in stabilization calculations using harmonic oscillator basis functions and in a recent modification of the stabilization method.[30]

E. Other continuum finite basis set methods

It will be clear from the analysis above that any method capable of producing the form of the continuum functions on a finite domain containing the range of the potential or the asymptotic phase shifts is, in principle, also capable of predicting the location and width of resonance lines. Probably the most widely known and most frequently used method available for this purpose is the R-matrix method originally developed by Wigner and Eisenbud.[2] Several more accurate variations of this basic method have been proposed more recently.[3,4,19,31–34] Apart from the fact that they apply to the time-independent Schrödinger equation and thus to energy dependence rather than directly to time dependence these methods are conceptually and computationally similar to the ABM. In fact, in the process of developing the ABM we have obtained several new variations of the R-matrix method which appear to be particularly efficient.[18,19] Thus we have extended this work to include an examination of the accuracy of the standard R-matrix method and two improved methods described in our earlier work[19] when applied to the prediction of location and width of a resonance line. We have also done Buttle[4] corrected R-matrix calculations but found difficulty in incorporating this method in our present density of states approach to resonance. It would, of course, be more suitable for a phase shift approach to resonance. The results of our calculations are reported in the following section.

III. RESULTS OF TEST CALCULATIONS

The test calculations using the methods discussed in Sec. II were carried out for the Hazi and Taylor (HT) potential[15]

TABLE II. Results of the ABM calculations for the HT potential and comparison with the exact resonance parameters $L_2 = 34.0$ in all calculations.

			SMA		ISMA		exact (Hazi and Taylor)[15]	
λ	L_1	$L_1-\Delta$	E_r	Γ	E_r	Γ	E_r	Γ
0.125	10.0	8.0	0.472 949	$0.1857E-4$	0.472 942	$0.3112E-4$	0.472 940	$0.3607E-4$
	9.75	7.75	0.472 955	$0.2891E-4$	0.472 945	$0.3569E-4$		
	9.50	7.50	0.472 961	$0.4058E-4$	0.472 946	$0.3633E-4$		
0.150	10.0	8.0	0.466 097	$0.1258E-3$	0.466 092	$0.2693E-3$	0.466 105	$0.3210E-3$
	9.75	7.75	0.446 140	$0.1273E-3$	0.466 118	$0.2509E-3$		
	9.50	7.50	0.466 174	$0.1358E-3$	0.466 123	$0.2420E-3$		
0.190	10.0	8.0	0.452 586	$0.1748E-2$	0.453 239	$0.2903E-2$	0.453 536	$0.2805E-2$
	9.75	7.75	0.453 029	$0.1314E-2$	0.453 271	$0.2339E-2$		
	9.50	7.50	0.453 270	$0.1015E-2$	0.453 261	$0.2219E-2$		
0.225	10.0	8.0	0.436 369	$1.0171E-2$	0.440 658	$1.0807E-2$	0.441 333	$0.8996E-2$
	9.75	7.75	0.438 039	$0.6121E-2$	0.440 006	$0.8814E-2$		
	9.50	7.50	0.438 813	$0.4216E-2$	0.439 848	$0.8462E-2$		
0.260	10.0	8.0	0.413 530	$0.3365E-1$	0.428 784	$0.2585E-1$	0.429 033	$0.1976E-1$
	9.75	7.75	0.418 826	$0.1825E-1$	0.425 708	$0.2294E-1$		
	9.50	7.50	0.420 614	$0.1199E-1$	0.425 103	$0.2257E-1$		

$$V(r) = \tfrac{1}{2} r^2 , \qquad r \leq 0$$
$$V(r) = \tfrac{1}{2} r^2 \exp(-\lambda r^2) , \qquad r \geq 0 \tag{38}$$

with $\lambda > 0$. In all calculations the basis sets consist of sine functions and the matrix elements of $V(r)$ were calculated by spline fitting the potential as piecewise cubic polynomials followed by piecewise integration. The number of subdivisions ranged from ~80 to 183, sufficient to have yielded results that converged completely. In all calculations the basis was localized on $[-5.0, L]$, penetrating sufficiently far into the classically forbidden region. Reduced units have been used throughout, i.e., $\hbar = m = 1$.

A. Stabilization method calculation

A stabilization calculation was carried out for the HT potential with $\lambda = 0.260$, performing five bound state calculations using successively larger basis sets with up to 100 sine functions on an interval $[-5.0, L]$. L was chosen so that each basis spanned the same energy range. In each calculation the full Hamiltonian matrix was diagonalized and the interior norms $\{I_l\}$ of the eigenvectors $\{\psi_l\}$ calculated,

$$I_l = \int_{L_0}^{L_B} dr |\psi_l|^2 , \quad l = 1, 2, \ldots, N , \tag{39}$$

where $L_0 = -5.0$ and $L_B (= 1.9612)$ is the position of the top of the barrier in $V(r)$. In Table I the results of the stabilization calculation are summarized listing the four eigenvalues that lie closest to the resonance energy $E_r = 0.4290$.

For $N = 20$, $L = 8.0$, as noted before, there is a single stable state within $\Gamma (\approx 0.02)$ of E_r and it is nearly completely localized on $[L_0, L_B]$. The lowest eigenstate is strongly localized on $[L_B, L]$, while the third state with energy just below the barrier height ($E_B = 0.7075$) is completely delocalized as are all higher states. For $N = 40$ and 60 essentially the same situation exists although the stable state has increased in energy while its interior norm has dropped to 0.69. For $N = 80$, $L = 47.0$ there are clearly two eigenvalues within Γ of E_r with comparable norms, i.e., destabilization has occurred. The trend is quite obvious, as N and L increase more states will appear near E_r, i.e., the resonance state will be spread over a number of bound eigenstates.

B. ABM calculations

The ABM calculations were carried out using the short memory approximation (SMA) and the improved short memory approximation (ISMA), as described previously.[12] The interior basis of 20 sine functions was localized on $[-5.0, L_1]$, the exterior basis consisted of 100 sine functions localized on $[L_1 - \Delta, L_2]$, where the parameters L_1, L_2, and Δ were chosen in accordance with our previous work.[12] The projection operators P and Q were defined so that P space is spanned by the interior functions orthogonalized to the exterior set. The matrix $\mathbf{H}_{eff}$ was set up in the interior basis that diagonalized $\mathbf{H}_B$, it is thus identified as $\{|\phi_l\rangle\}$ in (21) and (22). $\mathbf{H}_{eff}$ was evaluated at a time of 1.6, corresponding to the first minimum in the memory kernel $|A_{11}(T)|$.[12]

Table II summarizes the results of the ABM calculations for several values of λ in the HT potential. The resonance energy E_r and width Γ are simply the real and twice the imaginary part of the eigenstate of $\mathbf{H}_{eff}$ identified as the resonance state. For comparison the "exact" results of Hazi and Taylor are also listed. It is immediately obvious that the resonance energies are predicted to good accuracy by the ABM especially by the ISMA. The accuracy in the calculated widths is also satisfactory, again the ISMA results are the more accurate, generally within 25% of the exact values. Some dependence on the parameters is apparent however, especially when the SMA is used. More detailed tests revealed that the results were most sensitive to the choice of $L_1 - \Delta$ rather than L_1 or L_2. While this sensitivity is inconvenient it does not seem a serious problem. More extensive variation of the parameters revealed no

greater variation in the resonance energies and widths than what is already present in Table II. Increasing the interior and/or exterior basis sets had only marginal effects on the results. Since the ISMA results are more accurate as well as more consistent when compared with the SMA, it is probable that the errors in the ABM are caused by the Markoffian approximation made in evaluating $\mathbf{H}_{eff}$. We hope to eliminate some of these errors in a more accurate, future version of the ABM.

The identification of an eigenstate of $\mathbf{H}_{eff}$ as a resonance state is a straightforward task. A state with an eigenvalue that has a very small imaginary part and a real part below the barrier height and whose interior norm is close to 1.0 is most probably a resonance state. In case of broad resonances it may be necessary to calculate the projected density of states $\rho_B(E)$ according to (20)–(27) for a range of energies which then may be fitted to a Lorentzian line shape if such a fit is at all applicable. As an illustration, in Table III we have listed the ten lowest eigenvalues of a $\mathbf{H}_{eff}$ from an ABM calculation with the ISMA for $\lambda = 0.260$ in the HT potential together with the interior norms of the corresponding eigenvectors. There are three states that lie at lower energy than E_B, of which the third is obviously the resonance state since it is strongly localized in the interior region as well as having a small imaginary component in its eigenvalue. When $\rho_B(E)$ was calculated at 8–10 energies close to the expected resonance energy and the results fitted to a Lorentzian line shape we obtained $E_r = 0.429\,768$ and $\Gamma = 0.025\,61$, nearly the same values as originally predicted by reading off the real and imaginary components of the third eigenstate of $\mathbf{H}_{eff}$. In case of narrower resonances the identification of resonance states is even simpler, e.g., for the HT potential with $\lambda = 0.125$ there is only one eigenvalue with an imaginary component of 0.1816×10^{-4} (and real component 0.472 946, interior norm 0.9988), the next smallest imaginary component being 0.0111 (real component 1.315, interior norm 0.879). In the latter case fitting a Lorentzian to the calculated $\rho_B(E)$ values reproduced the same resonance parameters as already predicted.

Finally, in Fig. 3 a plot of $\rho_B(E)$ is shown as obtained from an ABM (ISMA) calculation and for comparison the corresponding near-exact plot obtained by application of the Bloch corrected R-matrix method (see Sec. III C) is also displayed. The Lorentzian curves representing the resonance line shapes are very similar, as expected, the ABM curve having the larger width ($\Gamma = 0.025\,61$) compared with the more accurate width of 0.01983 obtained by the Bloch corrected R-matrix method. Above E_B the exact $\rho_B(E)$ is expected to be a monotonically decreasing function of E, with possibly some broad structure superimposed on it due to the nonconstant potential. The curve from the Bloch corrected R-matrix calculations does behave in that way while considerably more structure is present in the ABM curve. The extra oscillations in the latter have been identified as artifacts of the finite basis and will be discussed in detail in future work.

TABLE III. The lowest eigenvalues of $\mathbf{H}_{eff}$, $\{E_l - i\lambda_l\}$, from an ABM (ISMA) calculation with corresponding interior norms $\{I_l\}$. λ of HT potential is 0.260.

E_l	λ_l	I_l
0.1143	0.0444	0.0018
0.4187	0.1159	0.0626
0.4288	0.0129	0.8046
0.8195	0.1371	0.0915
1.1801	0.0959	0.3751
1.5744	0.1167	0.3316
2.0850	0.1141	0.3638
3.2593	0.1095	0.4242
3.9240	0.1071	0.4722
4.6327	0.1051	0.4733

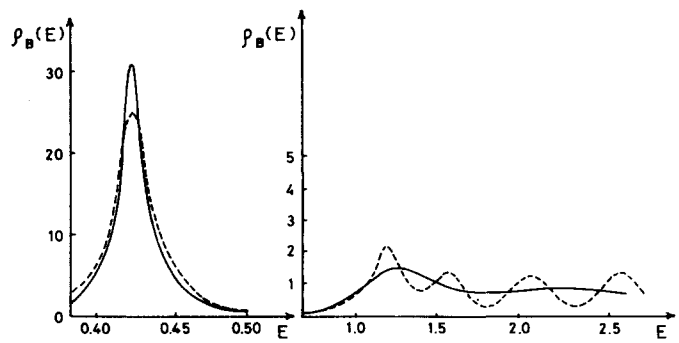

FIG. 3. Plots of the projected density of states, $\rho_B(E)$, obtained from an AMB (ISMA) calculation (broken lines) and a Bloch corrected R-matrix calculation (solid lines) for a Hazi and Taylor potential with $\lambda = 0.260$.

C. Continuum finite basis set calculations

The most straightfroward approach to obtain the projected density of states $\rho_B(E)$ is by calculating the exact, or highly accurate, continuum eigenstates to the time-independent Schrödinger equation at given energies E. Thus if $S(E, r)$ is an eigenstate with energy E and normalized according to (30),

$$\rho_B(E) = [(2m/E)^{1/2}/\hbar\pi] \int_{L_0}^{L_B} dr\, |S(E, r)|^2 \ , \tag{40}$$

where $[L_0, L_B]$ is the interval on which the density of states is projected by B. In a finite basis set calculation $S(E, r)$ is expanded as a linear combination of a suitable set of basis functions $\{\phi_l(r)\}$ localized in the region where $V(r) \neq 0$ and penetrating sufficiently into the classically forbidden region. Thus,

$$S(E, r) = A(E) \sum_l c_l \phi_l(r) \ , \quad L_0 \leq r \leq L \ , \tag{41a}$$

while in the asymptotic region

$$S(E, r) = \sin[(2mE)^{1/2} r/\hbar + \theta(E)] \ , \quad r \geq L \ , \tag{41b}$$

where $A(E)$ is the appropriate normalization constant.

The finite basis methods used in this work comprise the R-matrix method,[2] an improved version of it, which we have termed the Bloch corrected R-matrix method,[19] and one of the continuum generalized finite element methods, CGFEM III, recently developed by us.[19] The theoretical basis of all three methods has been discussed

TABLE IV. Results of continuum finite basis set calculations for the HT potential. (N = number of basis functions).

	CGFEM III ($N=20$)			R matrix ($N=20$)			R matrix ($N=40$)		
λ	E_r	Γ	A	E_r	Γ	A	E_r	Γ	A
0.125	0.472 940	0.3631$E-4$	1.0004	0.472 942	0.3398$E-4$	0.9998	0.472 941	0.3522$E-4$	0.9999
0.150	0.466 106	0.3222$E-3$	0.9974	0.466 105	0.2752$E-3$	0.9974	0.466 105	0.2976$E-3$	0.9973
0.190	0.453 579	0.2819$E-2$	0.9879	0.453 370	0.2663$E-2$	0.9848	0.453 461	0.2738$E-2$	0.9862
0.225	0.441 584	0.8840$E-2$	0.9766	0.441 051	0.9527$E-2$	0.9743	0.441 327	0.9229$E-2$	0.9760
0.260	0.429 956	0.1969$E-1$	0.9755	0.429 379	0.2294$E-1$	0.9946	0.429 713	0.2132$E-1$	0.9850
	Bloch corrected R matrix ($N=20+4$)			Bloch corrected R matrix ($N=40+5$)					
λ	E_r	Γ	A	E_r	Γ	A			
0.125	0.472 942	0.3655$E-4$	1.0000	0.472 940	0.3646$E-4$	0.9999			
0.150	0.466 108	0.3211$E-3$	0.9972	0.466 106	0.3205$E-3$	0.9972			
0.190	0.453 569	0.2816$E-2$	0.9877	0.453 570	0.2817$E-2$	0.9877			
0.225	0.441 561	0.8880$E-2$	0.9765	0.441 564	0.8875$E-2$	0.9765			
0.260	0.429 949	0.1983$E-1$	0.9762	0.429 951	0.1981$E-1$	0.9761			

in detail elsewhere.[2-4,18,19] As stated earlier we had difficulty implementing the Buttle corrected R-matrix method[4] in a density of states calculation since the Buttle correction readily applies to phaseshifts rather than to wave functions.

In the CGFEM III method the continuum eigenfunction is expanded on $[L_0, L]$ as

$$S(E,r)=A(E)\left\{[1-\exp(-a(r-L_0))]\times\cos[k(r-L)]+\sum_{l=1}^{N} d_l u_l(r)\right\}, \tag{42}$$

where

$$u_l(r)=(2/(L-L_0))^{1/2}\sin\frac{l\pi(r-L_0)}{L-L_0} \tag{43}$$

and

$$k=(2mE)^{1/2}/\hbar\ . \tag{44}$$

In the present calculations $L_0=-5.0$, $L=10.0$, $a=b/(L-L_0)$, $b=10.0$, $N=20$. The choice of b is not critical, near-identical results were obtained with $b=5.0$.

In the R-matrix method the expansion of $S(E,r)$ takes the form

$$S(E,r)=A(E)\sum_{l=1}^{N} c_l u_l(r) \tag{45}$$

with

$$u_l(r)=(2/(L-L_0))^{1/2}\sin\frac{(l-\frac{1}{2})\pi(r-L_0)}{L-L_0}\ , \tag{46}$$

while in the Bloch corrected R-matrix method the basis in (45) is extended by a few (3–5) localized sine functions so that

$$S(r,E)=A(E)\left\{\sum_{l=1}^{N} c_l u_l(r)+\sum_{l=1}^{n} d_l v_l(r)\right\}, \tag{47}$$

where

$$v_l(r)=(2/\Delta)^{1/2}\sin\frac{l\pi(r-L+\Delta)}{\Delta}\ ,\quad L-\Delta\leq r\leq L\ . \tag{48}$$

The number of basis functions, N, in the basic R matrix expansion was 20 and 40, while the number of additional functions, n, in the Bloch corrected R-matrix method was 4–5 with $\Delta=1.5$.

Using the three continuum methods described above $\rho_B(E)$ was evaluated at a number of energies in a direct search for the resonance peak. Consequently it is very easy to miss a resonance, especially if it is narrow, in direct contrast with the ABM approach. Once the rough position of the resonance was located $\rho_B(E)$ was calculated at 8–10 points within $\pm\Gamma$ of E_r which were then fitted to a Lorentzian curve,

$$\rho_B(E)=A\,\frac{1}{\pi}\,\frac{\Gamma/2}{(E-E_r)^2+(\Gamma/2)^2} \tag{49}$$

using a least squares procedure. Thus three parameters were determined for a given resonance peak, where the value of A indicates the quality of the fit. $A=1$ for an exact Lorentzian fit. Any departure from that value is an indication of errors in $\rho_B(E)$ or the presence of some non-Lorentzian character in the resonance line shape.

The results in Table IV confirm our expectations of the various methods. CGFEM III and the Bloch corrected R-matrix method perform very well, the two methods yielding results in excellent agreement. The standard R-matrix results are considerably poorer although significant improvement was obtained when the basis was increased to 40 functions. A similar increase in basis had negligible effect on the CGFEM III and the Bloch corrected R-matrix results. In fact, we have not included the CGFEM III results with $N=40$ in this article. Comparison with the Hazi and Taylor[15] exact E_r and Γ values (see Table II) indicates fairly close agreement although some of the differences that are present are certainly greater than what we can ascribe to numerical or basis set errors. Some disagreement is to be expected since the methods used here and those of Hazi and Taylor calculate the resonance parameters differently. Hazi and Taylor have obtained the E_r and Γ values by fitting the calculated phaseshifts to the Breit–Wigner formula (11) and as we have already pointed out

it is impossible to completely separate the resonant part of the phaseshift from the background, $\eta_{pot}(E)$. In our approach such a separation was made naturally using the spatial projection technique on the density of states. Thus we ascribe some of the differences between the two sets of results to the slight contribution of states localized outside the barrier ($r > L_B$) to the density of states in the calculations of Hazi and Taylor.

We may conclude this section with the observation that continuum finite basis set methods are well suited to the study of resonances and are capable of giving very accurate numerical information.

IV. CONCLUSION

The main conclusion of this work is that, as anticipated on conceptual grounds, the ABM works also for tunneling decay although in its present forms it is not as accurate in resolving the corresponding narrow lines as are the best of the continuum methods, e.g., the CGFEM and the Bloch corrected R-matrix method. It would appear that the ABM copes more readily with time dependent properties. Even for energies allowing rapid decay accurately reproduced by the ABM the corresponding density of states tends to oscillate around the correct value. We plan to address this problem in greater detail in a future publication. It is clear, however, that since time and energy dependence are related to each other by a Fourier transformation, a sufficiently accurate description of the time dependence will produce any desired accuracy in the description of the corresponding energy dependence.

We believe the advantages of the density of states analysis used above are worthy of note. Not only does this approach produce a very straightforward connection between rate theory and scattering theory but it would appear to be useful in other fields, e.g., statistical mechanics, as well. The relevance to the calculation of photoionization and photodissociation rates has been discussed in a preceding article.[13]

ACKNOWLEDGMENTS

We wish to thank M. A. Hooper for providing us with the Lorentzian fitting program for the density of states and for helpful discussions. This work was supported by the Australian Research Grants Committee.

APPENDIX: DERIVATION OF THE PROJECTED DENSITY OF STATES

The result (29) for the projected density of states $\rho_B(E)$ is readily obtained by first considering the case when the overall domain is of finite length L. In that case we have

$$\rho_B(E, L) = \sum_{l=1}^{\infty} \langle \phi_l | B\delta(H - E) | \phi_l \rangle \ , \tag{A1}$$

where $\{\phi_l\}_1^\infty$ is the normalized set of energy eigenfunctions. We now take the limit as $L \to \infty$ and note that in this limit

$$\phi_l(r) \to (2/L)^{1/2} S(k, r) \ , \tag{A2}$$

$$S(k, r) = \sin(kr + \theta(k)) \ , \quad r \to \infty \ , \tag{A3}$$

$$k = \pi l / L \ . \tag{A4}$$

Since the k values become infinitely dense the sum over l values can be replaced by an integration over k values. Setting dk equal to $dl\pi/L$ from (A4) we then find

$$\lim_{L\to\infty} \rho_B(E, L) = (2/\pi) \int_0^\infty dk \, \langle S(k) | B\delta(E(k) - E) | S(k) \rangle \ . \tag{A5}$$

So far the proof has proceeded in a manner similar to the derivation of the Fourier transform from the corresponding Fourier series expansion. It must be noted that the relation (A4) for the density of k values in the $L \to \infty$ limit holds even in the presence of a potential as long as its range is finite. We have also neglected the possibility of bound states.

In order to obtain the result (29) we note that in the $L \to \infty$ limit the energy is purely kinetic,

$$E(k) = \hbar^2 k^2 / 2m \ , \tag{A6}$$

$$k = (2mE/\hbar^2)^{1/2} \ . \tag{A7}$$

Changing variables to E we then get from (A5) the result

$$\begin{aligned} \rho_B(E) &= (2/\pi)(2m/\hbar^2)^{1/2} \int_0^\infty dE' \, \tfrac{1}{2}(E')^{-1/2} \\ &\quad \times \langle S(E') | B\delta(E' - E) | S(E') \rangle \\ &= [(2m/E)^{1/2}/\pi\hbar] \langle S(E) | B | S(E) \rangle \ . \end{aligned} \tag{A8}$$

Using the definition (28) of the projection operator B, we get

$$\rho_B(E) = \rho(E) \int_{L_0}^{L_B} dr \, |S(E, r)|^2 \ , \tag{A9}$$

where the total density of states (not normalized) is as given in (31).

[1] P. L. Kapur and R. Peierls, Proc. R. Soc. London Ser. A **166**, 277 (1937).
[2] E. P. Wigner and L. Eisenbud, Phys. Rev. **72**, 29 (1947).
[3] C. Bloch, Nucl. Phys. **4**, 503 (1957).
[4] P. J. A. Buttle, Phys. Rev. **160**, 719 (1967).
[5] R. P. Bell, *The Proton in Chemistry* (Cornell University, Ithaca, 1973).
[6] M. D. Harmony, Chem. Soc. Rev. **1**, 211 (1972).
[7] P. H. Cribb, S. Nordholm, and N. S. Hush, Chem. Phys. **29**, 43 (1978).
[8] J. M. Blatt and V. P. Weisskopf, *Theoretical Nuclear Physics* (Wiley, New York, 1952).
[9] J. R. Taylor, *Scattering Theory* (Wiley, New York, 1972).
[10] M. S. Child, *Molecular Collision Theory* (Academic, London, 1974).
[11] S. Nordholm and S. A. Rice, J. Chem. Phys. **62**, 157 (1975).
[12] S. Nordholm and G. Bacskay, J. Chem. Phys. **70**, 2497 (1979).
[13] S. Nordholm, J. Chem. Phys. **71**, 2313 (1979).
[14] C. J. Joachain, *Quantum Collision Theory* (North-Holland, Amsterdam, 1975), Sec. 4.5.
[15] A. U. Hazi and H. S. Taylor, Phys. Rev. A **1**, 1109 (1970).
[16] I. Eliezer, H. S. Taylor, and J. K. Williams, J. Chem. Phys. **47**, 2165 (1967).
[17] H. S. Taylor, *Advances in Chemical Physics*, Vol. 18, edited by I. Prigogine and S. A. Rice (Interscience, New York, 1970), p. 91.
[18] S. Nordholm and G. Bacskay, Chem. Phys. Lett. **42**, 259 (1976).
[19] S. Nordholm and G. Bacskay, J. Phys. B **11**, 193 (1978).
[20] M. A. Hooper and S. Nordholm, Chem. Phys. (in press).
[21] U. Fano, Phys. Rev. **124**, 1866 (1961).

[22]F. H. Mies and M. Krauss, J. Chem. Phys. **45,** 4455 (1966); F. H. Mies, *ibid.* **51,** 787 and 798 (1969); Phys. Rev. **175,** 164 (1968).
[23]L. Mower, Phys. Rev. **142,** 799 (1966).
[24]T. G. Waech and R. B. Bernstein, J. Chem. Phys. **46,** 4905 (1967); R. J. Le Roy and R. B. Bernstein, *ibid.* **54,** 5114 (1971).
[25]R. I. Price, Mol. Phys. **33,** 559 (1977).
[26]J. O. Hirschfelder, C. F. Curtiss, and R. B. Bird, *Molecular Theory of Gases and Liquids* (Wiley, New York, 1964), Sec. 1.7.
[27]P. W. Langhoff, Int. J. Quant. Chem. Symp. **11,** 301 (1977) and references cited therein.
[28]S. Nordholm, J. Electron Spectrosc. Relat. Phenom. **15,** 109 (1979).
[29]P. H. Cribb, S. Nordholm, and N. S. Hush, Chem. Phys. **29,** 31 (1978); Proceedings of the Conference on Tunneling in Biological Systems (Philadelphia, November, 1977) (to appear).
[30]J. F. Liebman, D. L. Yeager, and J. Simons, Chem. Phys. Lett. **48,** 227 (1977).
[31]D. J. Zwijac, E. J. Heller, and J. C. Light, J. Phys. B **8,** 1016 (1975).
[32]R. F. Barrett and P. P. Delsanto, Phys. Rev. C **10,** 101 (1974).
[33]S. S. Ahmad, R. F. Barrett, and B. A. Robson, Nucl. Phys. A **257,** 378 (1976); **270,** 1 (1976).
[34]E. J. Heller and H. A. Yamani, Phys. Rev. A **9,** 1201 (1974).